Eng. & Technology, Vol.24, No.8, 2005

Calculation of The Electrons Distribution Function For Mercury –Argon Mixture

Ibrahim G. Faiadh,* F. L. Rasheed,* Hamid B. Mahood*

Received on: 1/3/2004
Accepted on: 6/10/2005

Abstract

The electron energy distribution in mercury-argon mixture discharge calculated numerically from the Boltzmann equation. In this job The mixture parameters such as drift velocity, excitation rates and ionization coefficient are calculated which are plotted as a function of the E/N. Values of the ratio of the electric field, E to the gas number density, N of interest in this work are in the range from 10^{-18} to 10^{-14} V. cm^2.

The results show a good agreement with available experimental and theoretical data. The present results are relevant for the modeling of discharges in argon which its atoms play a major role in the kinetics of various lasers.

حساب دالة توزيع الإلكترونات لمزيج من بخار الزئبق و غاز ألا ركون

الخلاصة

تم حساب دالة توزيع طاقة الإلكترونات في تفريغ مزيج من بخار الزئبق و غاز ألا ركون عدديا من معادلة بولتزمان. في هذا العمل تم حساب أيضا معلمات إضافية مثل سرعة الجرف ، معدلات التهيج و معامل التأين و التي تم رسمها كدالة لـ E/N (نسبة المجال الكهربائي E إلى الكثافة العددية للغاز N) ، حيث أن مداه يتراوح من 10^{-18}إلى 10^{-14} فولت . سم2 .

أظهرت النتائج التي تم الحصول عليها تطابقا جيدا مع المعطيات العملية و النظرية المتوفرة ، والتي تكون مناسبة لنمذجة التفريغ في غاز ألا ركون حيث أن ذراته تلعب دورا مهما في حركيات الليزرات المتنوعة.

Nomenclature:

The symbols and their units are as follows:

u	Electron energy (eV)
E	Electric field (V m^{-1})
m	Electronic mass (kg)
M	Atomic mass (kg)
k	Boltzmann's constant (JK^{-1})
T_g	gas temperature (K)
e	electronic charge (C)
ε_0	Permittivity of free space (F m^{-1})
N	neutral density (m^{-3})
N_e	electron density (m^{-3})
T_e	electron temperature (K)
N_j	number density of th jth state (m^{-3})
Q_j	cross-section of the jth process (m^2)
Q_{-j}	cross-section for the reverse of the jth process (m^2)
u_j	Threshold energy of the jth process (eV)
Q_m	momentum transfer cross-section (m^2)

* Ministry of Science & Technology, Baghdad-IRAQ.

https://doi.org/10.30684/etj.24.8A.8
2412-0758/University of Technology-Iraq, Baghdad, Iraq

Introduction

In laser gas modeling, the pumping rates are usually calculated. From the electron energy distribution function which is obtained by solving numerically the steady state homogenous Boltzmann , the reason for this is that the gas in the discharge is only weakly ionized and the electron energy distribution, began dominated by the electron-neutral collisions, may be highly non-Maxiwellian.The main collision types which is include elastic, in elastic, super-elastic and electron Coulomb collisions are considered in such analyses [1-22].

At the range gas pressure, the calculated electron energy distribution has been found to have depletion at the region above the effective excitation energy threshold. This characteristic has also been showing by independent experimental investigations using the Druyvestyn second differential method. The depletion characteristics in the distribution can case large error in the pumping rate calculations if a Maxwellian distribution is used instead.

To calculate the electron energy distribution, numerous data have to be compiled from the literature to be fed in to Boltzmann equation coputation.Althogh the solution method of the equation may be Accurate the solution depends heavily in the accuracy of the input data.There is no indications that what is calculated represents the actual distribution in the discharge, especially if the discharge is in pulse mode.In this paper,an attempt is made to compare the electron energy distribution calculated from steady-state homogenous Boltzmann equation with the experimental data[23].

Boltzmann equation:

The general electron distribution function F is given by the steady state Boltzmann equation

$$\nabla_r \cdot \overline{v}\, F + \nabla_v \cdot \frac{e\bar{E}F}{m} = C(F)$$

The terms on the left-hand side are the divergences in configuration and velocity spaces and C(F) is the collision operator.

Homogeneous Boltzmann equation:

Following the usual expansion, the isotropic component(u) of the spatially independent electron energy distribution in a uniform electric field is given by the equation below [24].

$$\frac{d}{du}\left(H(u)\frac{df}{du}(u) + J(u)f(u) \right) =$$

$$\sum_j [(u+u_j)f(u+u_j)NQ_j(u+u_j) - uf(u)NQ_j(u)]$$

$$+ \sum_j [(u-u_j)f(u-u_j)NQ_{.j}(u-u_j) - uf(u)NQ_{.j}(u)]$$

where

$$H(u) = \frac{uE^2}{3NQ_m(u)} + \frac{2mu^2}{M}\frac{kT_g}{e}NQ_m(u) + Q_{ee}A_1(u)$$

$$J(u) = \frac{2mu^2}{M}NQ_m(u) + Q_{ee}A_2(u)$$

$$Q_{ee} = \frac{4\pi\pi^4 N_e}{(4\pi 4\pi_0)^2}\ln\left(\frac{12\pi 2\pi_0 T_e)^{3/2}}{N_e^{1/2}e^{3/2}}\right)$$

$$A_1(u) = \frac{4\pi}{3mN_e}\left(\frac{2}{m}\right)^{3/2}\left(\int_0^u u^{3/2}f(u)du + u^{3/2}\int_u^\infty f(u)du\right)$$

$$A_2(u) = \frac{4\pi}{mN_e}\left(\frac{2}{m}\right)^{1/2}\int_0^u u^{1/2}f(u)du$$

The normalization of this distribution is :

$$2\pi\left(\frac{2e}{m}\right)^{3/2}\int_0^\infty u^{1/2}f(u)du = N_e$$

on the right-hand side,the first summation is due to the excitation processes and the second summation is due to the reverse processes. The ionization process has been treated as an excitation process without a reverse process. The terms,Qee,$A_1(u)$and$A_2(u)$are due to electron –electron Coulomb processes.

The electron energy distribution has been assumed to be nearly isotropic, thus allowing it to represented by a two-term spherical harmonic expansion. This condition is satisfied at reasonably low values of E/N where the drift speed is much less than the random speed.

The momentum loss in the coulomb collision has also been neglected .This is valid if the electron-electron collision frequency is much less than the electron-atom collision frequency. In weakly ionized gas discharges where $Ne/N<10^{-4}$.Renormalising the equation by letting

$$f_0(u) = \frac{2\pi}{N_e}\left(\frac{2e}{m}\right)^{3/2} f(u)$$

We have

$$\int_0^\infty u^{1/2}f_0(u)du = 1$$

The equation remains the same form except that f(u) is replaced by $f_0(u)$ and $A_1(u)$ and $A_2(u)$ become

$A_1(u)=$

$$\frac{1}{3}\left(\frac{m}{e}\right)^2\left(\int_0^u u^{3/2}f_0(u)du + u^{3/2}\int_u^\infty f_0(u)du\right)$$

$$A_2(u) = \frac{1}{2}\left(\frac{m}{e}\right)^2\int_0^u u^{1/2}f_0(u)du$$

The transport parameters are defined as follows. The drift velocity,$V_d$is

$$V_d = -\frac{E}{3}\left(\frac{2e}{m}\right)^{1/2}\int_0^\infty \frac{u}{NQ_m}\frac{df_0}{du}du$$

The rate of jth process is

$$R_j = \left(\frac{2e}{m}\right)^{1/2}\int_0^\infty uNQ_j f_0 du$$

Numerical method:

The equation is written in its difference form and solved by Gauss elimination and and Gauss-Siedal iteration [25]. The boundary conditions are set by imposing particle conservation within the energy range considered and an energy balance calculation is used to check the solution. The energy gained per second from the electric field and super elastic collisions is:

$$V_dE + \sum_j u_j R_{-j}$$

where R_{-j} is the rate of super elastic collisions .The energy lost per second through elastic, excitation and ionization collision is

$$(2m/M)\,\bar{u}\,R_{el} + \sum_j u_j R_j$$

where $R_{el}$is the of elastic collision and R_j are the rates of excitation and ionization collisions.

The results and conclusion:

Fig (1-3) show the energy distribution function for the mercury-argon mixtures have been computed at E/N values 2, 20, and 200 Td, respectively, this show the value of the distribution function at the electrons energy of 5 eV is larger. This, of course, in means that there is possibility for the electrons to carry out inelastic collisions at low E/N values in the case of pure mercury vapor[23]. It is observed that as the concentration of mercury vapor decrease in the mixture, the more inelastic collisions is expected to occur with the increase of the E/N values. As shown in figures (1-3) that the distinct increase in the distribution function is observed at low electron energy regions as compared with other regions. This indicates to the region of the increase number of electrons which lost their energy due to inelastic collision and fall down to the low energy region. Of course, this assures the decrease of the E/N values with the decrease of mercury vapor concentration at the occurrence of the inelastic collisions. The direct effect of this behavior is on the values of electron transport parameters.

Fig (4) show the behavior of ν_d for the first three mixtures above is similar to that of pure mercury vapor except at E/N value where v_d starts to increase with the increase of E/N at the value of 1 Td approximately. A comparison of figure (4) with figure (5), it is noticed that the inelastic collision between the electrons and the atoms and/or molecules of the mixture starts at E/N ~1Td. This indicates that in such mixture an increase in drift velocity ν_d is obtained. While in the above last three mixtures, the same behavior is found except of unsimilarity in the behavior at E/N<1 Td and E/T>100 Td and this unsimilarity increases with decrease of mercury vapor concentration in the mixture. This behavior is clearly observable in figures (6-8), respectively. In these figures, as the concentration of mercury vapor decreases, the value of E/N decreases where there is an inelastic collision. This causes an increase in the number of low energy electrons as indicated in the description of the energy distribution function. This behavior leads to a decrease in the electrons velocity at these low energy regions. At high energy regions, the difference in the behavior is due to the decrease of E/N value at which the ionization process starts for mercury vapor atoms. Of course, in the ionization process, the decrease in the energetic electrons occurs because of the capture of electrons by mercury vapor atoms or due to the loss of electrons as a result of their energy transfer to the mercury atoms as a result of inelastic collisions. This transfer will leave the electrons with very low energy which leads to a decrease in the number of energetic electrons according to the above we can say : when the concentration of Hg vapor increasing and decreasing the concentration of Ar , at this instant , there are stable in elastic collision following fall like sharp , but happen the opposite , there are falling sharp , and when increasing in Ar and deceasing in Hg , there are falling in the fractional power like following case [23].

The excitation rate behavior for all electronic levels is approximately similar to the case of pure mercury vapor. The difference is in the value of E/N at which the excitation rate starts to increase with the increase of E/N value for each electronic level

and most the electrons energy transfer to the second electronic level up to a specified E/N value which depends according to the type of mixture as shown in figures (9-13). The electronic levels gain their energy according to E/N value such as the case of energy transfer to the $6\,^3p_2$ and $6\,^1p_1$ levels. However, the values of E/N are different and they depend on the type of mixture.

It is observed that comparison of the figures (12-13) with the figures (7-8) shows that the fractional powers of the electronic excitation and the ionization have fixed values. This behavior is accompanied by fixed values of the excitation rates for the four electronic levels at E/N>100 Td. This means that the system reached the stable state and that most of the energy will transfer to $6\,^1p_1$ level and then to other levels $6\,^3p_0$, $6\,^3p_1$, $6\,^3p_2$, respectively. In this case that at high E/N values, the electrons energy increases to the value that the electrons are ready to excite all the levels even the ionization state in mercury vapor atoms. However, as mentioned previously, this depends on the cross sections for the four electronic levels and the cross sections for ionization.

Fig (14) the behavior of ionization coefficient as a function of E/N.The value of ionization coefficient increases with the decrease of mercury vapor concentration in the mixture. As E/N value increases, the differences in ionization coefficient values decreases down to the value at which they are approximately meeting at one point. This behavior is due to the increase in the number of electrons that causing the ionization as the mercury vapor concentration decreases in the mixture. This is interpreted as in the case of pure mercury vapor, the energetic electrons collide in elastically with mercury atoms losing their energies and become at low energy. In the mixture with low mercury atoms concentration, an excess in the number of energetic electrons is found as a result of the decrease in the number of mercury atoms in the mixture. As E/N value increases, these electrons will acquire an extra energy and their number that causing ionization will increase with the decrease of the mercury atoms. A comparison of figure (14) with figures (5-8) shows that the final values are fixed at higher E/N values for all mixtures. This behavior is related to the stability of ionization state and also to the electronic excitation. This indicates that whatever to be the difference in mixture ratios there are a limited number of electrons which initiate the ionization in the mercury atoms at specified E/N values. Of course, the ionization process depends on the ionization cross sections. The distribution function approaches the Maxwell-Boltzmann distribution function at higher E/N values [26]. In such situation of the distribution, the numbers of electrons with relatively high energy are limited and this explains why the values of ionization coefficients for different mixtures meet at one point when E/N value increases.

References

1. Jochen Kronjaeger, Gas Discharge with a Rotary Vacuum Pump, Internet, file://A:\pump.htm, (2000-2002).
2. Ibrahim Gittan Faiedh, et.al, J. Saddam University Science, Vol.6 (1) 52-60(2002).

3. Paul A. Tiple, Physics for scientists and engineers, fourth ed. W. H. Freeman Comp. U.S.A, (1999).
4. Narciso Garcia & Afthur Damask, Physics for computer science students, Springer-Verlage, New York, Inc. U.S.A (1991).
5. Grant B. Gustafon & Calvin H. Welcox advanced engineering mathematics, Springer-Verlage, New York, Inc. U.S.A (1998).
6. Matthew N.0. Sadiku, Elements of Electromagnetic, Third Edition, Oxford University Press, Inc., U.S.A, (2001).
7. Phys J., D: Appl. Phys. Vol. 11,337 (1978).
8. Frost L S., Phelp, AV, Phys. Rev., 127, 1621-33, (1962).
9. Morgan W.L., B.M. Penetrane, Computer Physics Communications CPC, Vol.58, 127-152(1990).
10. Rockwood S.D., Green A. E., Computer Physics, Communication, 19, 377, (1980).
11. Crompton R. W., Gibson D.K., McIntosh A .I., Aust. J. Phys., 22, 715 (1969).
12. Boris M. Smirnov, Physics of Ionized Gases, John Wiley and Sons, Inc., New York, (2001).
13. Wedding A.B., J.Phys. D: Appl.Phys. Vol.18, 2351-2359, (1985).
14. Aust. J. Phys., , 33, 231-50, (1980).
15. J. Phys. D: Appl. Phys., 17 (1984) 1159-1166. Printed in Great Britain.
16. Johnson T H, Palumbo L. J., Hunter II A M IEEE J.Quantum Electron. QE-15 289-301, (1979).
17. Long W. H., Jr Appl. Phys. Lett. 31, 391-4, (1977).
18. Frost L S and Phelps A V (1964) Phys.Rev. A 136 1538-45.
19. Puech V., Torchin L., J.Phys. D: Apple. Phys. 19, 2309 – 2323, (1986).
20. Loureiro J., Ferreira C. M. , J. Phys. D:Apple. Phys. 22, 67-75, (1989).
21. Ushirodo S., Kajita S., Kondo Y., J. Phys., D:Apple. Phys. 23, 47-52, (1990).
22. Ibrahim Gittan Faiedh, Dr. Raad Hameed J. College of Education for women, 13, 1, 99, (2002).
23. Phys. Rev. A, Vol.8, (5), 2348, (1973).
24. Frost L. S., Phelps A. V. Phys. Rev. A 136 1538-45. (1964).
25. Thomson R M, Smith K., Davies A. R., Comp. Phys. Commun.11, 369-83, (1976).
26. B.E. Cherrington, Gaseous Electronics and Gas Lasers, Pergamon Press, (1979).

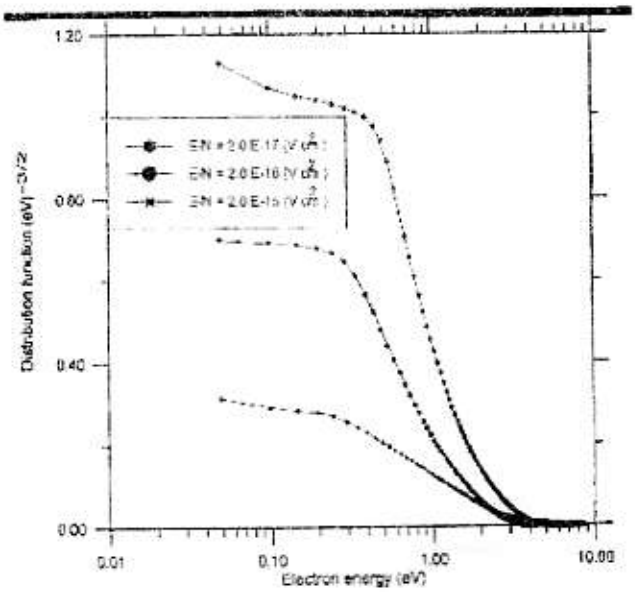

Fig(1) : The electron distribution function versus the electron energy in Hg-Ar mixture (45% Hg ,55% Ar)

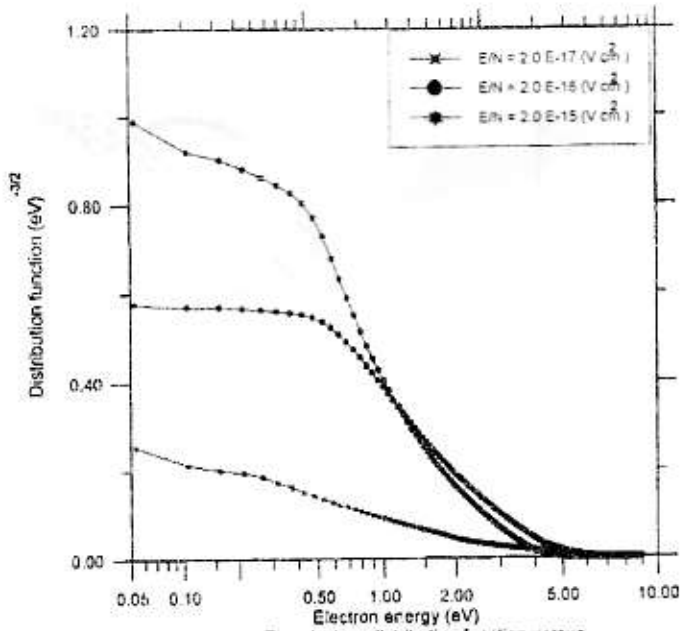

Fig(2) : The electron distribution function versus the electron energy

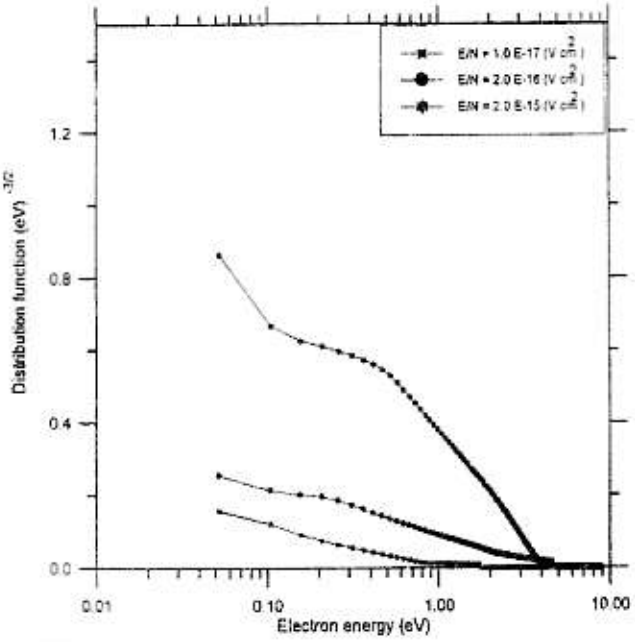

Fig(3) : The electron distribution function versus the electron energy in Hg-Ar mixture .(5% Hg ,95% Ar).

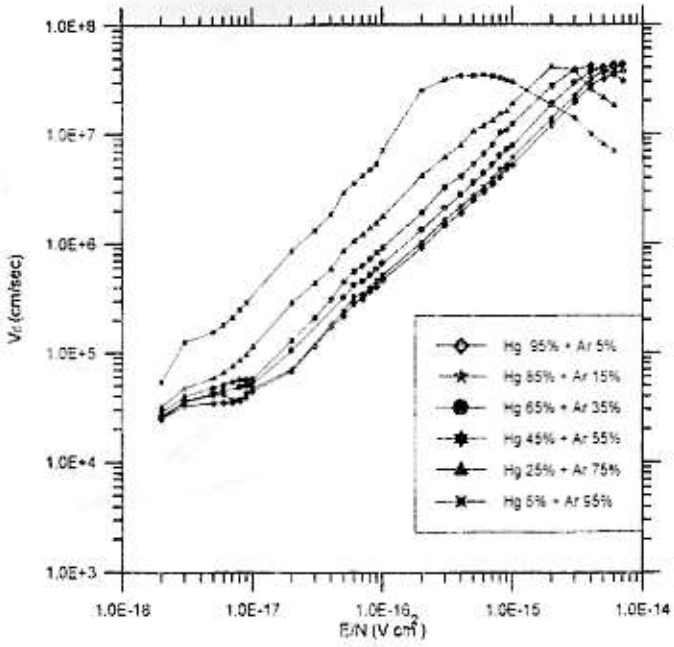

Fig(4) :The electron drift velocity versus E/N in Hg-Ar mixture .

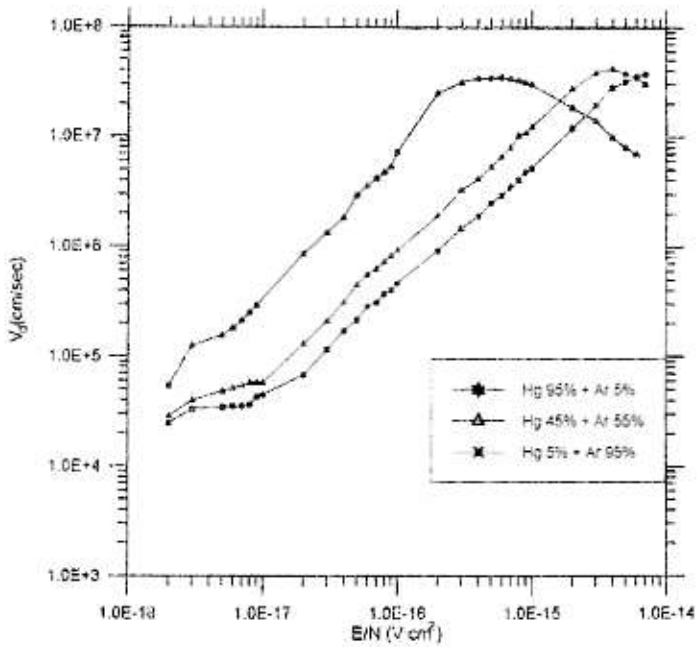

Fig(5) The electron drift velocity versus E/N in Hg-Ar mixture .

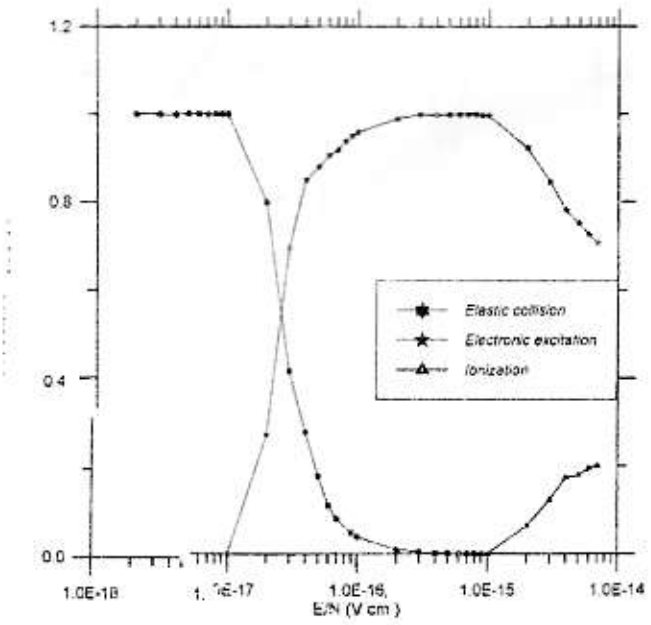

Fig(6) :The fractional partitio[illegible] of total discharge power versus E/N in mixture H_g-Ar (65% ,35%) .

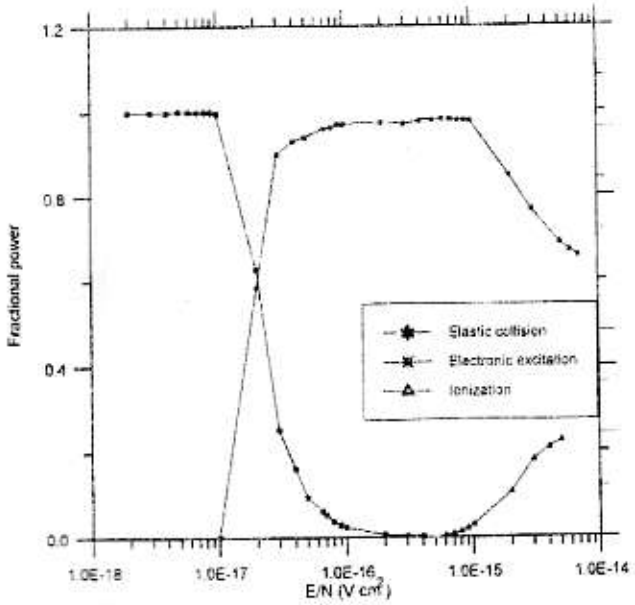

Fig(7):The fractional partition of total discharge power versus E/N in Hg-Ar mixture (45% Hg , 55% Ar)

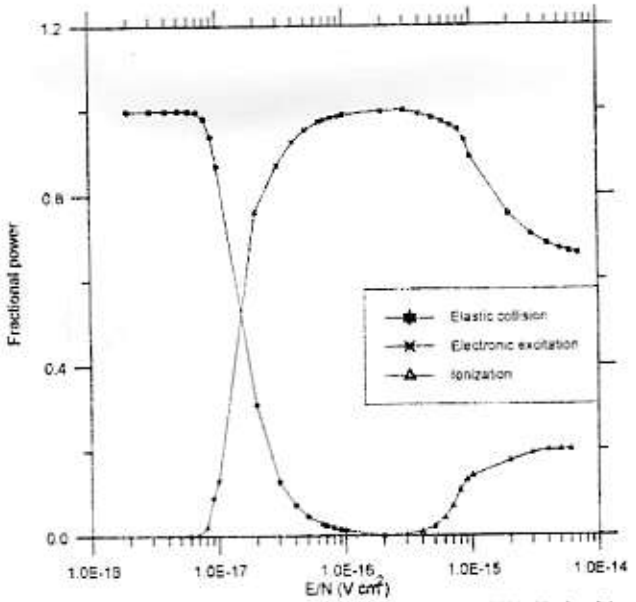

Fig(8) : The fractional partition of total discharge power versus E/N in Hg-Ar mixture (25% Hg ,75% Ar).

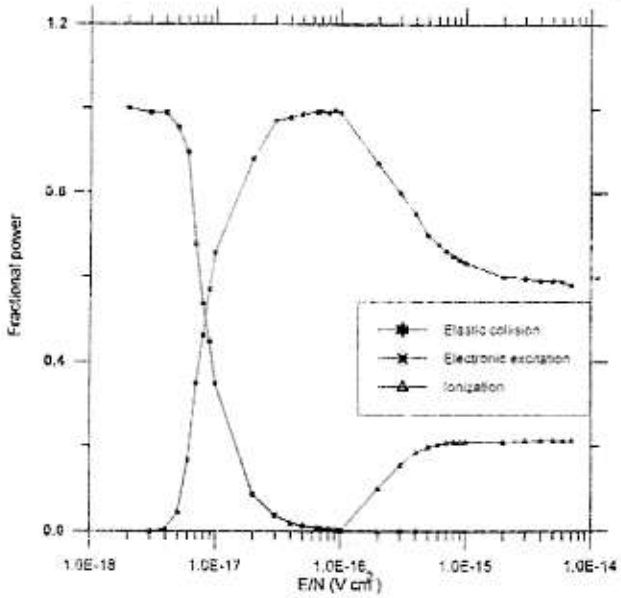

Fig(9) : The fractional partition of total discharge power versus E/N in Hg-Ar mixture (5% Hg ,95% Ar).

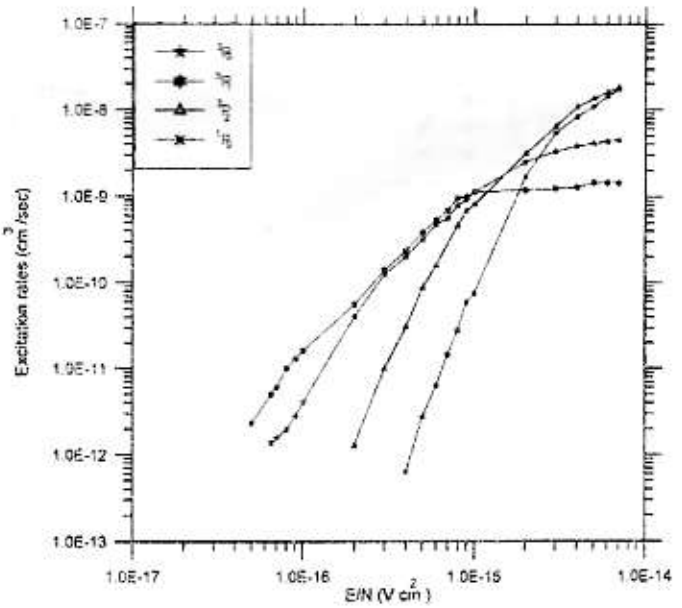

Fig(10) : The computed excitation rates to selected excited states versus E/N for Hg in Hg-Ar mixture .(85% Hg , 15% Ar) .

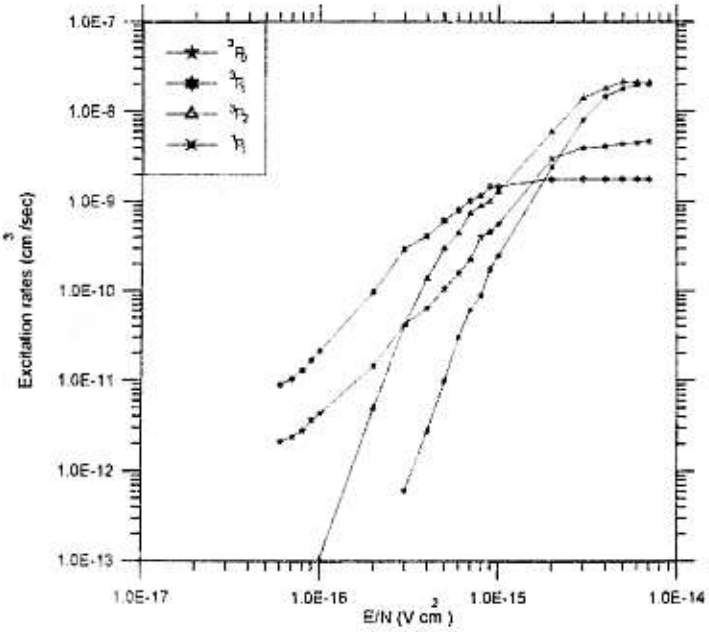

Fig(11): The computed excitation rates to selected excited states versus E/N for Hg in Hg-Ar mixture , (65% Hg , 35% Ar).

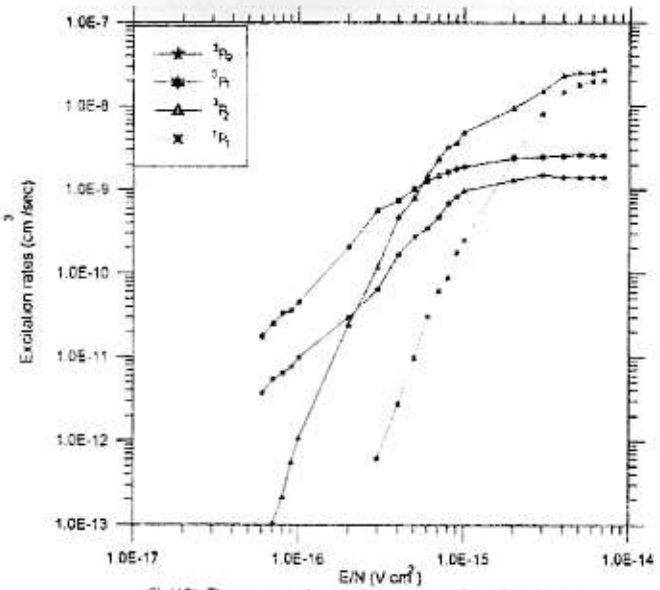

Fig(12): The computed excitation rates to selected excited states versus E/N for Hg in Hg-Ar mixture , (45% Hg , 55% Ar)

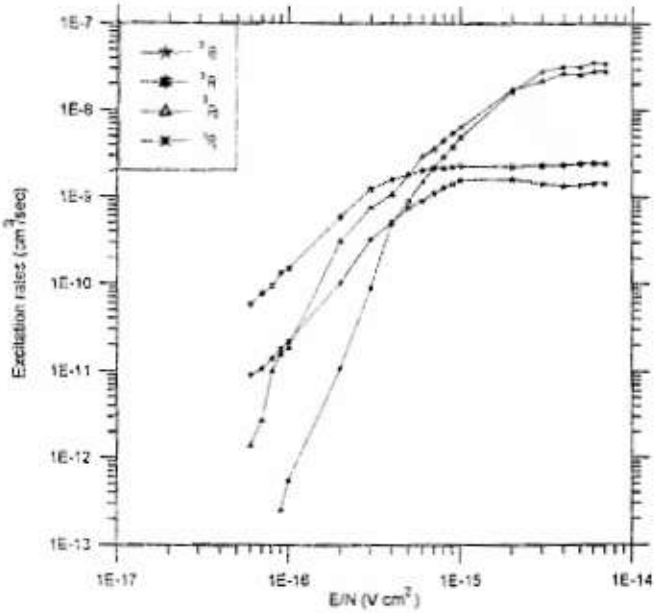

Fig(13): The computed excitation rates to selected excited states versus E/N for Hg in Hg-Ar mixture (25% Hg , 75% Ar).

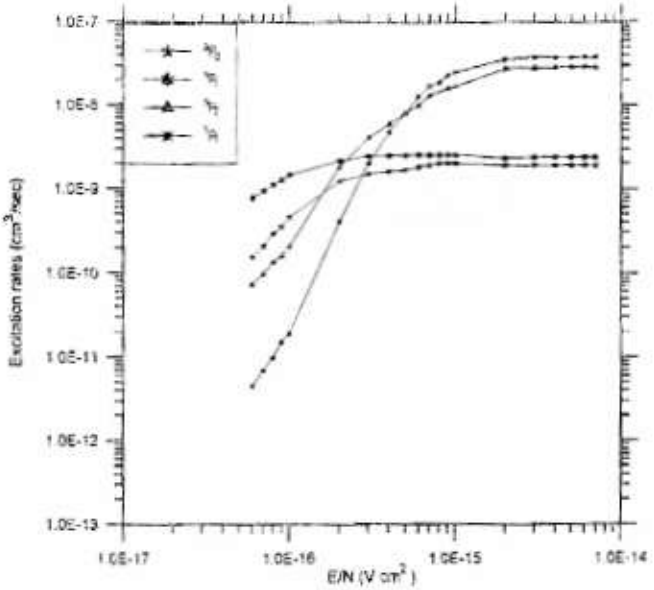

Fig(14): The computed excitation rates to selected excited states versus E/N for Hg in Hg-Ar mixture , (5% Hg , 95% Ar).

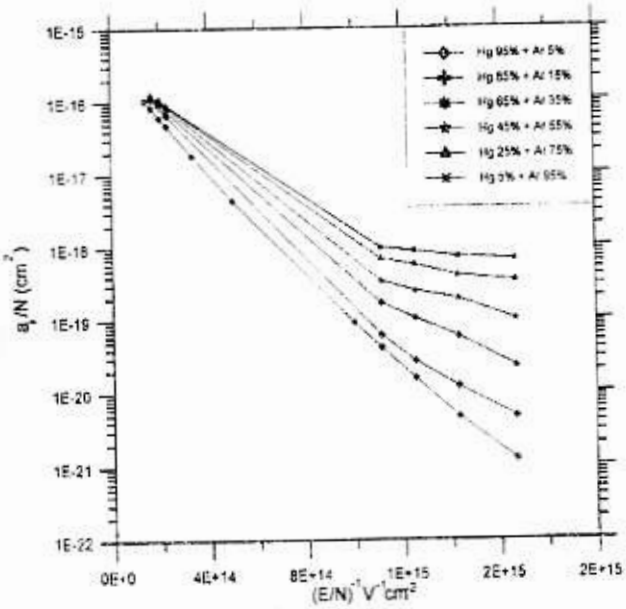

Fig(15): The ionization coefficient per molecule versus (E/N)$^{-1}$ in Hg-Ar mixture